

Galerkin methods for numerical solutions of acoustic, elastic and viscoelastic wave equations

Matt A. McDonald, Michael P. Lamoureaux, Gary F. Margrave

ABSTRACT

The numerical modelling of wave equations is a common theme in many seismic applications, and is an important tool in understanding how the physical systems of interest react in the process of a seismic experiment. We apply state-of-the-art numerical methods based on domain-decomposition combined with local pseudospectral spatial discretization, to three physically realistic models of seismic waves, namely their propagation in acoustic, elastic, and viscoelastic media. The Galerkin formulation solves the weak form of the partial differential equation representing wave propagation and naturally includes boundary integral terms to represent free surface, rigid, and absorbing boundary effects. Stability, accuracy, and computation issues are discussed in this context along with direct comparison with finite difference methodologies.

This short paper is a summary of highlights from the 2012 MSc thesis of the first author, which aims to bridge the gap between the development of accurate physical models to represent the real world, as seen in seismic modelling, and the implementation of modern numerical techniques for the accurate solutions of partial differential equations.

INTRODUCTION

The numerical modelling of seismic waves is an integral part of many seismic processing procedures. When attempting to image the subsurface of the earth it is sometimes necessary to iteratively update the current model based on the difference between the response of the modelled system, and the data recorded from the actual experiment. As such, it is important that both the numerical method, and the type of model used in the forward modelling are capable of accurately representing the physical experiment.

Here, an argument is made that the partial differential equations that accurately model the earth's properties require a specific type of numerical method. More precisely, because of the discontinuous nature of the earth's properties, the partial differential equations exhibit a low-order level of continuity that shows as a "kink" at the discontinuous interfaces. Approximation methods that assume a higher level of continuity, can cause the position of these kinks to show up at incorrect spatial locations, leading to improperly reconstructed earth models.

In conducting the research for this work, the main motivation came from two previous works. The main source, was that of E. Faccioli, F. Maggio, R. Paolucci and A. Quarteroni which culminated in the papers Faccioli et al. (1996, 1997). Their work laid the general framework for a high-order numerical method based on domain-decomposition combined with pseudospectral methods, and included a boundary treatment based on Lagrange multipliers that made it extremely efficient to model semi-infinite media by implicitly enforcing the boundary conditions as part of a damping term.

Several years later the work of Faccioli et al. was reproduced independently by D. Komatitsch and J.-P. Vilotte in Komatitsch and Vilotte (1998), using a different method for time-advancement.

VERSIONS OF THE WAVE EQUATION

The full acoustic wave equation for pressure is written as

$$\ddot{u}(\mathbf{x}, t) = K(\mathbf{x}) \nabla \cdot \left(\frac{1}{\rho(\mathbf{x})} \nabla u(\mathbf{x}, t) \right) + f(\mathbf{x}, t), \quad \mathbf{x} \in \Omega, t > 0, \quad (1)$$

where K is the bulk modulus, ρ is the density of the media and f is the forcing term. Ω is the domain, which is assumed to be discontinuous globally, but made up of smaller continuous sections where waves will have constant parameters. $x \in \mathbb{R}^d$, $d = 1, \dots, 3$ is the spatial dimension, dot denotes the time derivative and ∇ is the gradient operator. This simulates a pure pressure wave propagating through the region Ω and has only a single component u representing the pressure in the medium at a point \mathbf{x} at time t .

The elastic wave equation is obtained by replacing pressure with a vector valued displacement function $\mathbf{u} = (u_1, \dots, u_d)$ defined on an isotropic heterogeneous medium $\Omega \subset \mathbb{R}^d$, with a vector valued forcing function $\mathbf{f} = (f_1, \dots, f_d)$. The d-components of the differential system are expressed as

$$\rho(\mathbf{x}) \ddot{u}_i(\mathbf{x}, t) = \sum_j \frac{\partial}{\partial x_j} \sigma_{ij}(\mathbf{u}) + f_i, \quad \mathbf{x} \in \Omega, t > 0, i = 1, \dots, d, \quad (2)$$

where the stresses for the isotropic medium are

$$\sigma_{ij}(\mathbf{u}) = \lambda(\nabla \cdot \mathbf{u}) \delta_{ij} + \mu \left(\frac{\partial}{\partial x_i} u_j + \frac{\partial}{\partial x_j} u_i \right), \quad (3)$$

with λ, μ the elastic parameters for the medium. It is physically significant that in this case, the density ρ is outside the derivative, while the elastic parameters λ, μ are inside the derivative, which leads to different qualitative behaviour when these parameters are not constant.

In the viscoelastic case, the material response to stresses becomes time-dependent; the Kelvin-Voigt model for this behaviour uses springs and dash-pots to represent this physical case. In our model of the wave equation, the results in a modification to the definition of stress, with

$$\sigma_{ij}(\mathbf{u}) = \lambda(\nabla \cdot \mathbf{u}) \delta_{ij} + \mu \left(\frac{\partial}{\partial x_i} u_j + \frac{\partial}{\partial x_j} u_i \right) + \lambda' \nabla \cdot \mathbf{v} \delta_{ij} + \mu' \frac{\partial}{\partial t} \left(\frac{\partial}{\partial x_i} u_j + \frac{\partial}{\partial x_j} u_i \right), \quad (4)$$

where \mathbf{v} is velocity (the time derivative of displacement \mathbf{u}) and λ', μ' are additional viscoelastic parameters.

The reader is referred to Carcione et al. (2004) for details on the viscoelastic model.

GALERKIN METHODS FOR SOLVING THE WAVE EQUATION

The Galerkin method can be thought of as the Calculus of Variations performed backwards. That is, instead of solving the strong form of the problem as a differential equation, the Galerkin method seeks to find the weak form expressed in terms of integrals, and solve that instead.

To apply the method to a differential equation of the form $L[u] = f$, defined on a region Ω where L is a linear spatial differential operator, a space of functions V is chosen in which element u and v will reside. The function u is then written as a linear combination of the basis functions of the space,

$$u = \sum_i a_i \phi_i, \quad (5)$$

and v is chosen from amongst the basis functions. The measure of the residual $R[u] = L[u] - f$ should then theoretically be zero. That is,

$$\int_{\Omega} R[u]v \, dx = 0, \text{ for all } v \in C_0^1(\Omega), \quad (6)$$

or,

$$\sum_i a_i \int_{\Omega} L[\phi_i]\phi_j \, dx = \int_{\Omega} f\phi_j \, dx, \text{ for all } j. \quad (7)$$

For certain problems, where the strong form corresponds to the Euler-Lagrange equations of minimum potential energy, the Galerkin method is equivalent to a Rayleigh-Ritz minimization technique .

To make this a feasible numerical method, the infinite sums must be truncated at some large N , the integrals evaluated, and re-written as a large N -dimensional system of equations to be solved for the unknown a_i 's,

$$K\mathbf{a} = \mathbf{f}. \quad (8)$$

Clearly, the method is greatly dependent on how the choice of basis function affects the solvability of the resulting matrix equation. Choosing the basis functions to be sines or cosines (depending on the boundary conditions) would make the matrix K diagonal, so long as the differential operator is of the form of a constant coefficient DE.

Another method arises from choosing the basis functions to be compactly supported piecewise polynomials designed to control the bandwidth of the matrix. These are termed basis-splines or b-splines. The functions themselves are considered global, but are defined by a small set of nodes corresponding to the order of the basis function.

In computing the time evolution of a wave propagating through a medium, it is convenient to treat time and space separately. In this formulation, we obtain a large, N -dimensional system of ordinary differential equations to solve, in the form with initial conditions

$$M\ddot{\mathbf{u}} + K\mathbf{u} = 0, t > 0, \quad (9)$$

$$\mathbf{u}(0) = \mathbf{u}_0, \quad (10)$$

$$\dot{\mathbf{u}}(0) = \mathbf{u}_1, \quad (11)$$

where M is called the mass matrix, and K the stiffness matrix. These matrices will be computed from the particular wave equation under study, and will differ depending on the choice of basis functions for the Galerkin method, as well as choice of boundary conditions.

NODES

A key idea in this approach is that the basis functions are determined by their point-wise values on nodal points in space, from which their numerical derivatives and integrals can be computed directly. The nodal points are not uniformly spaced, in order to avoid Runge's phenomena where errors could accumulate near the boundary. For instance, Figure 1 demonstrates the problems that arise as we attempt to approximate a Gaussian using polynomials as basis functions, with uniformly distributed nodal points. As the number of nodes increases, the approximation gets worse and worse near the endpoints.

The fix is to choose Gauss-Lobatto points, as shown in Figure 2, which clusters the points near the boundaries. In this case, an optimal approximation of the Gaussian is obtained.

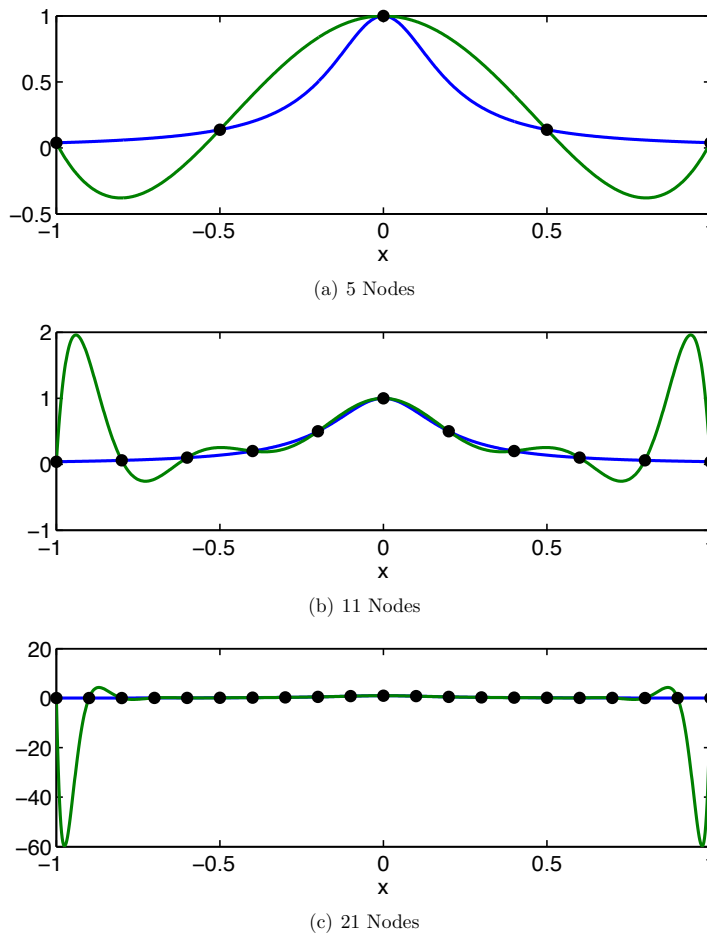


FIG. 1. Runge phenomenon for increasing order of interpolation. The blue line is the function, and the green line is the interpolating polynomial.

The Gauss-Lobatto points can be computed numerically. The region under study can

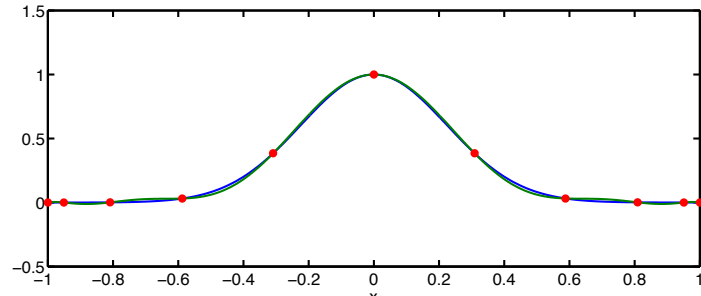


FIG. 2. Interpolation of the function $\exp(-10x^2)$ on clustered nodes.

be partitioned into different intervals, and Gauss-Lobatto points selected for each interval. In 2D, a rectangular domain is partitioned into sub-rectangles, and grids of Gauss-Lobatto points formed, as demonstrated in Figure 3. Observe the clustering near the centre lines; it will be useful to have many points near regions of discontinuity in the propagating medium.

The mathematical formulation, going from the nodes to basis functions to numerical derivatives and integrals (quadrature) are contained in the thesis of the first author, McDonald (2012).

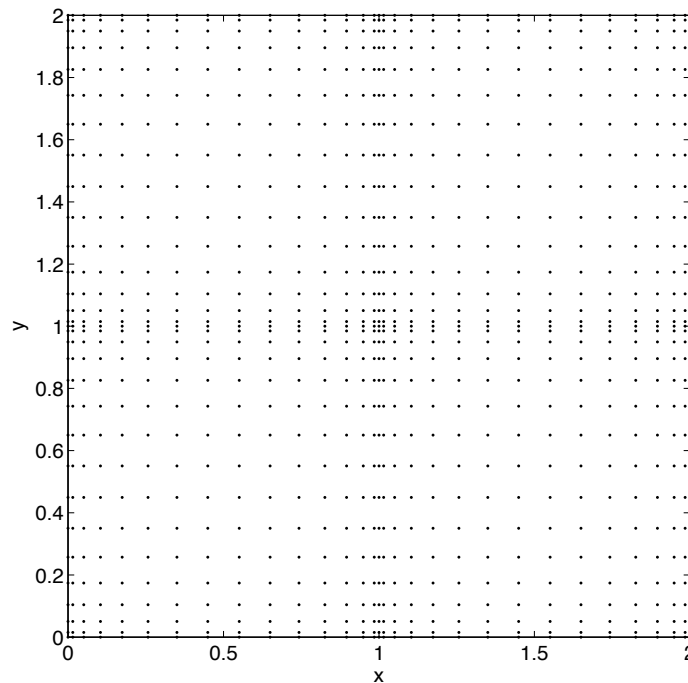


FIG. 3. 2D Legendre-Gauss-Lobatto SEM nodes distributed over 4 subdomains.

ABSORBING BOUNDARY CONDITIONS

The weak form (as integrals) of the wave equation that arises in the Galerkin formulation makes its very easy to translate boundary conditions into surface integrals, that can be directly incorporated into the numerical methods for solving the associated linear system representing the differential equations model. We have experimented with several

variations of boundary conditions (full reflection, Rayleigh boundary reflection, Higdon absorbing boundaries) to test the weak formulation as an implementation technique.

In Figure 4 one observes that the boundary reflections from the absorbing boundary conditions are zero along horizontal and vertical lines away from the source and increase as the angle of incidence increases, but the reflected wave has only about 10% of the energy of the incident wave. This is promising, however the increased computational cost may not be feasible for larger models.

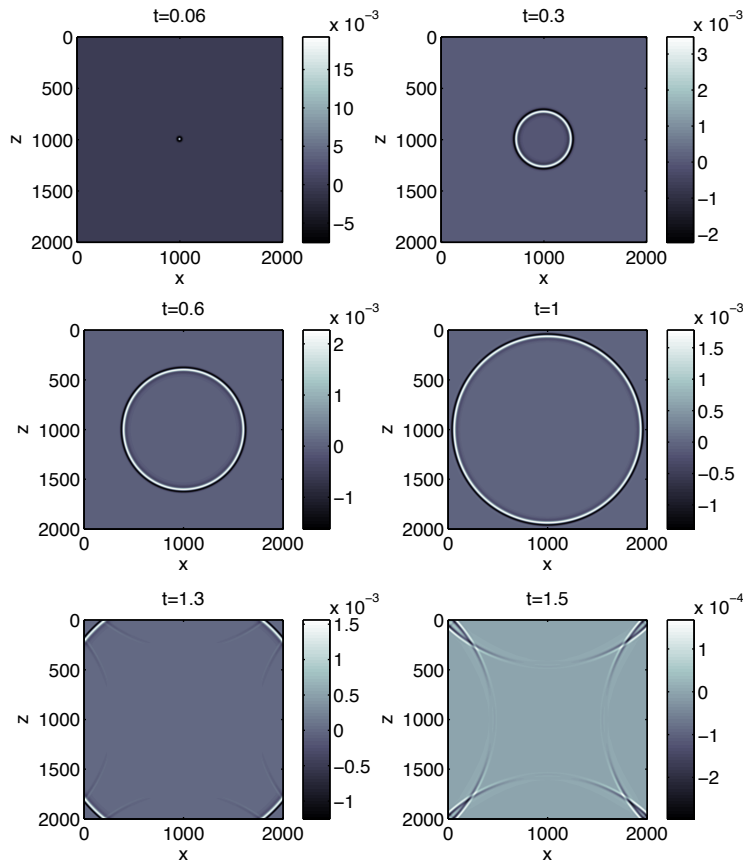


FIG. 4. Absorbing boundary reflection. Note the scale change.

GALERKIN COMPARED TO FINITE DIFFERENCE METHODS

A nodal Galerkin method is compared to fourth and second order finite difference methods on a 501 by 501 node grid. To test this we consider a forcing term with Ricker wavelet time-component and conservative spatial component

$$(u_1(x), w_1(x)) = -\nabla e^{-r\|x-x_0\|^2} \quad (12)$$

and propagate a 15 Hz wavelet in a 4500m square bipartite medium with properties $\rho = 2.064g/cm^3$, $V_p = 2305m/s$, $V_s = 997m/s$ in the first layer, and $\rho = 2.14g/cm^3$, $V_p = 4500m/s$, $V_s = 2600m/s$ in the second layer.

Figures 5, 6, 7 show the norm of the displacement for the three models propagated to one second and then normalized and clipped to exaggerate the dispersion effects. The

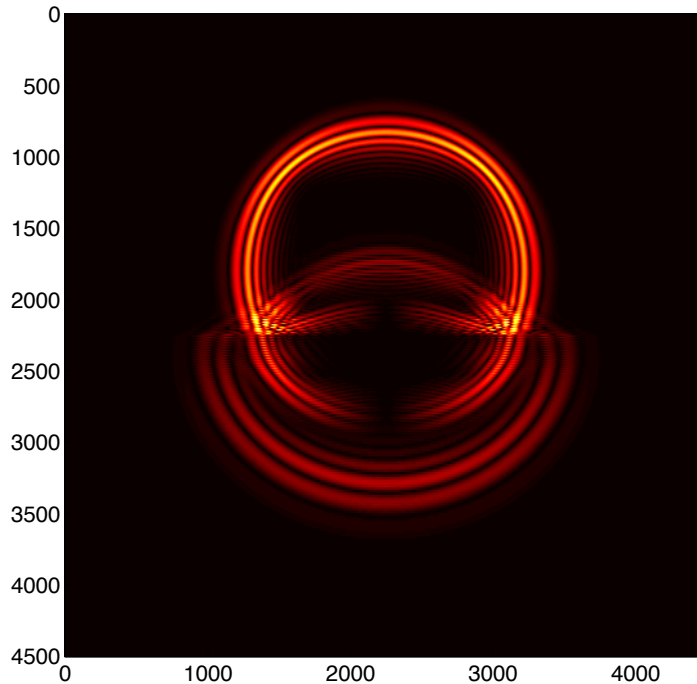


FIG. 5. Second-Order Finite Difference. Comp time = 64 s.

extended arcs in the fourth-order model result from the wider stencil moving over the large step in the velocity model and then being propagated. Again, this is exaggerated here and is mainly due to the relatively small number of grid points we are using, but the effect is apparent.

The computation times are listed with the figures but are not very indicative of the associated computation costs of the three methods. The implementation of the three methods are nearly identical, with the only difference being the application of the derivative approximations. For the finite-difference methods the cost of this is kN^2 where k is the width of the finite-difference stencil (3 for second order, 5 for fourth order). The differentiation matrices for the nodal Galerkin methods can be considered finite-difference matrices with stencils of width N and so the cost of applying these methods is N^3 . We take $dt = 0.0008$ and so take 1179 steps to reach one second. We could take a smaller time step, but the one chosen assures us that the wavelet in time is well-represented and that the error associated with time stepping will not taint our results as we are more interested in spatial accuracy.

Locally the fourth order model approximates the wavefronts better than the second-order model (as is expected), but the size of the stencil means that we must alter it somehow at the boundaries, this is not the case with the differentiation matrices that appear in the nodal Galerkin methods as they are global and so for the approximation of the derivative at one node they take information from all other nodes in the model.

Figures 8 and 9 show comparisons of the centerline of the model ($x = 2250$, for all z) at time corresponding wavefront in various regions of the velocity model. The amplitude error associated with the second-order stencil is apparent as is the dispersion of all three methods near a jump. Notice the ringing in Figure 9 that is apparent for both finite difference results.

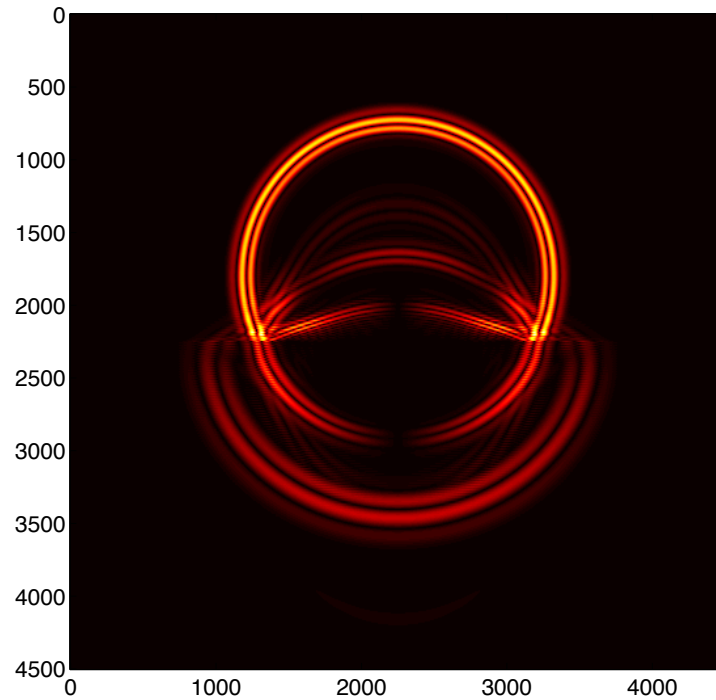


FIG. 6. Fourth-Order Finite Difference. Comp time = 75 s.

ELASTIC AND VISCOELASTIC SOLUTIONS

To demonstrate the utility of the Galerkin method used with accurate physical models, a comparison is made between wave propagation of a single impulse through a two-layer elastic medium and through a two-layer viscoelastic medium with damping parameters $Q_p = 24$, $Q_s = 16$, shown in Figure 10. Observe the viscoelastic model contains much more detail about the wave propagation, including physically relevant effects such as the broadening of the wavelength as it propagates.

FURTHER WORK

In terms of the numerical implementation of the methods in this research, some preliminary work was done with 3D modelling but not enough to warrant inclusion. Some research level software packages do exist for 3D pseudospectral-element modelling, but are more geared towards global-scale seismic modelling (see SPEC-FEM3D available at <http://www.geodynamics.org/cig/software/specfem3d>). It would be interesting to attempt to build attempt to replicate three-component three-dimensional seismic acquisition for a 2D line by restricting one of the horizontal dimensions to something small and then seeing if the absorbing boundary conditions properly handle the reflections from the relatively near boundaries. Another approach would be to assume a model that was constant in one spatial dimension and then analytically integrate the equations along that dimension to produce a 2.5D model. Both of these approaches could then be compared to a full 3D model and see if the results along the surface are similar. If so, this would lead to more accurate amplitudes in the modelled data and increase the computational efficiency drastically.

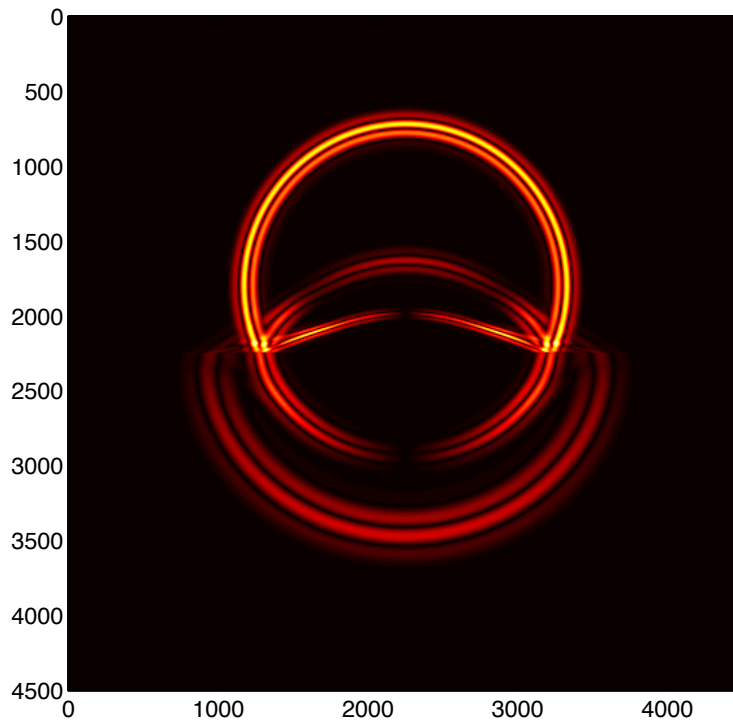


FIG. 7. Nodal Galerkin. Comp time = 206 s.

CONCLUSIONS

The research showed that the study of a Galerkin method is a feasible and computationally efficient method for the numerical modelling of several types of seismic waves. Special attention was paid to the treatment of numerically imposed boundaries and discontinuous interfaces through the use of the weak form of the dynamic equilibrium equations. Further, it was shown that a significant amount of analytic work is required to build the equation used in the numerical procedure, but that the payoff for such work is a more efficient model that is capable of representing desirable properties such as free-surface and absorbing boundary conditions with less input from the end-user.

Extended details are available in the thesis of the first author, McDonald (2012).

ACKNOWLEDGEMENTS

The authors gratefully acknowledge the financial support of NSERC, Mprime, PIMS, and the industrial sponsors of the POTSI and CREWES projects at the University of Calgary.

REFERENCES

- Carcione, J. M., Poletto, F., and Gei, D., 2004, 3-D wave simulation in anelastic media using the kelvin-voigt constitutive equation: *J. Comput. Phys.*, **196**, 282–297.
- Faccioli, E., Maggio, F., Quarteroni, A., and Tagliani, A., 1996, Spectral-domain decomposition methods for the solution of acoustic and elastic wave equations: *Geophysics*.

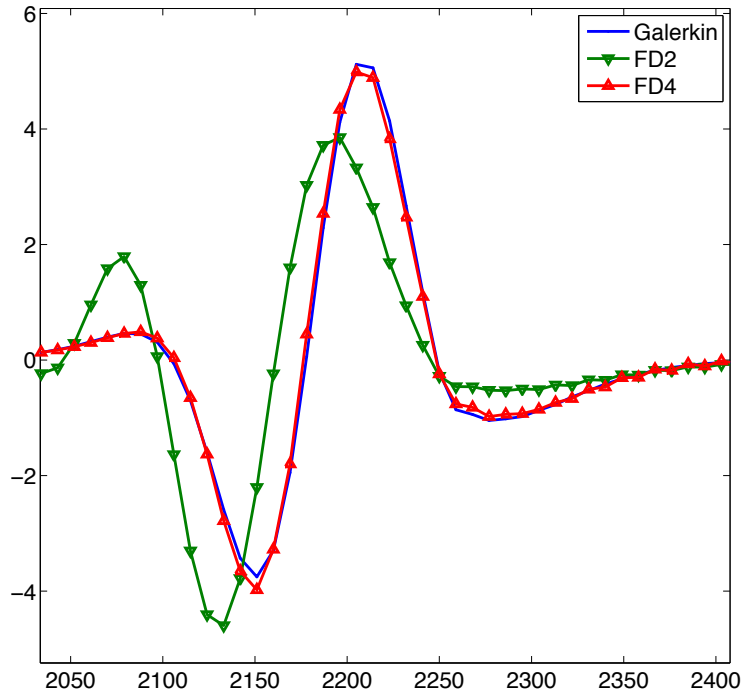


FIG. 8. Close-up of the centerline of the horizontal component of a 2D elasticwave. The region plotted shows the disagreement of the three methods in a smooth region of the velocity model.

Faccioli, E., Maggio, F., Quarteroni, A., and Tagliani, A., 1997, 2d and 3d elastic wave propagation by a pseudo-spectral domain decomposition method: *Journal of Seismology*, **1**, 237–251.

Komatitsch, D., and Vilotte, J., 1998, The spectral element method: An efficient tool to simulate the seismic response of 2d and 3d geological structures: *Bulletin of the Seismological Society of America*.

McDonald, M. A., 2012, Numerical methods in seismic wave propagation: University of Calgary MSc thesis.

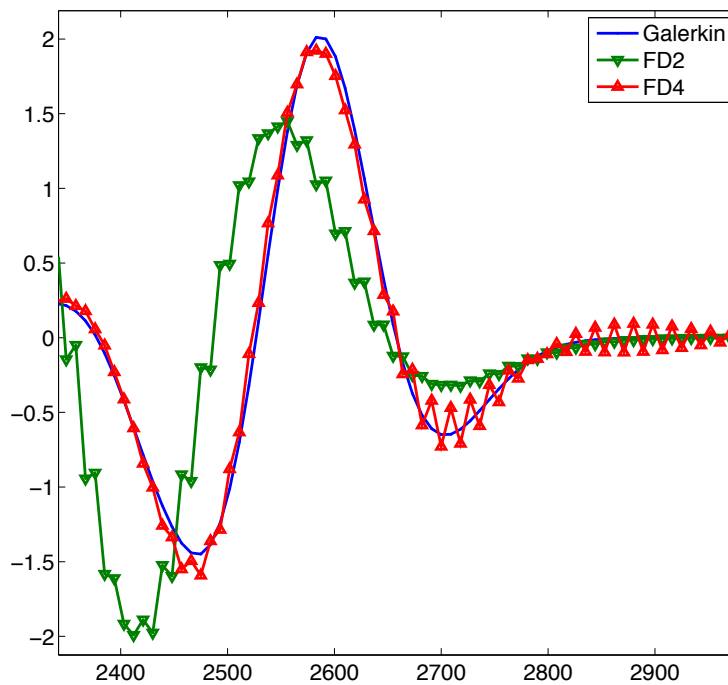


FIG. 9. Close-up of the centerline of the horizontal component of a 2D elastic wave. The region plotted shows the disagreement of the three methods in the presence of a sharp jump in the velocity model. Note the ringing in the FD methods.

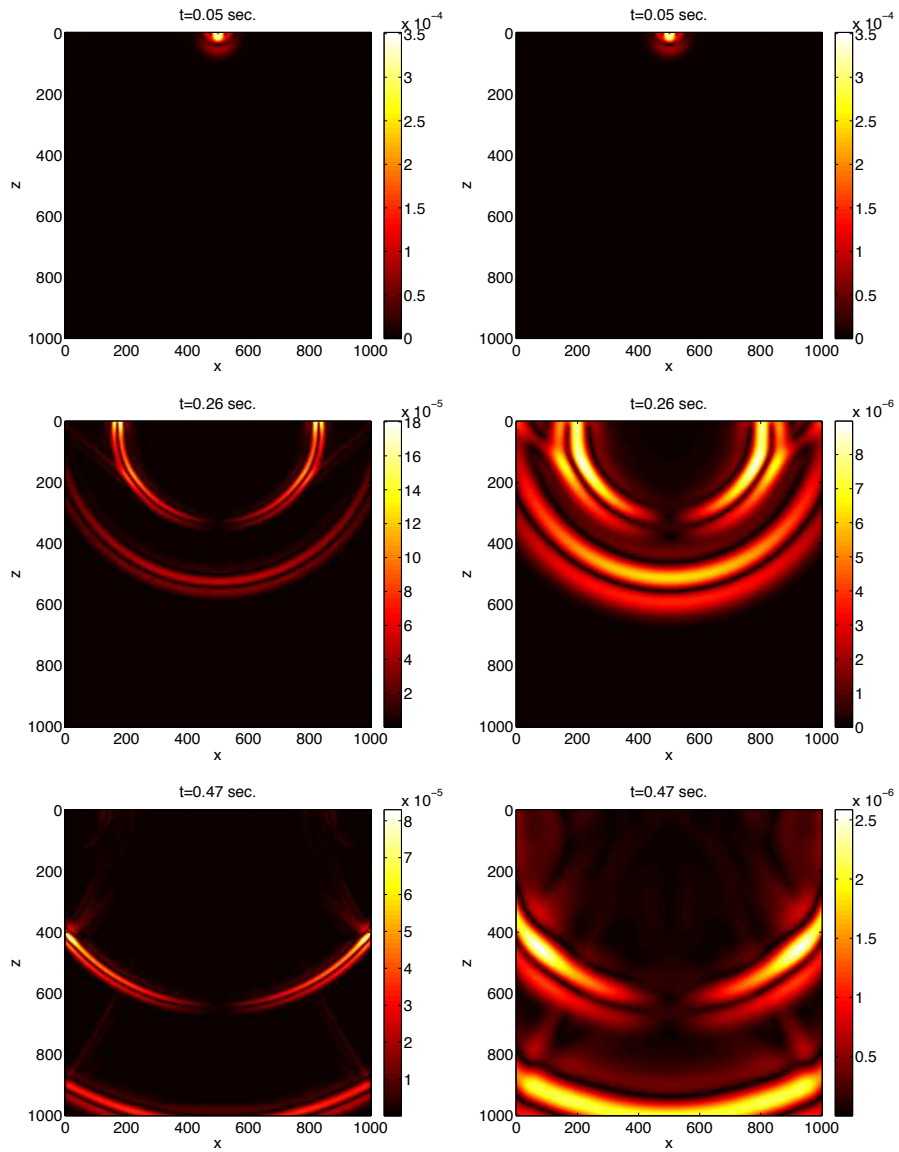


FIG. 10. Elastic vs. viscoelastic wave propagation.